

SYMPOSIUM ON FUEL CELLS  
PRESENTED BEFORE THE DIVISION OF PETROLEUM CHEMISTRY  
AMERICAN CHEMICAL SOCIETY  
CHICAGO MEETING, September 3-8, 1961

THEORY OF POLARIZATION OF POROUS  
GASEOUS-DIFFUSION ELECTRODES

By

H. B. Urbach  
Research Laboratories, United Aircraft Corporation  
East Hartford, Connecticut

INTRODUCTION

The decay of polarization at the interface between a flat-plate electrode and the adjacent electrolyte has been treated analytically by Grahame (1) and Scott (2). These authors have pointed out that formidable computational difficulties are involved in the determination of kinetic parameters from experimental data because of concentration changes which occur at the interface. However, Grahame (1) has shown that approximate solutions which reveal the major characteristics of the problem can be obtained with the aid of certain simplifying assumptions. The polarization-time curve for the limiting case in which the concentration polarization is zero has been calculated by Grahame, but his results show an extremely rapid decay of the polarization which is not verified by experimental observations of systems in which concentration polarization occurs.

The problems associated with a theoretical treatment of the porous gaseous-diffusion electrode can be expected to be even more complex than those for the flat plate due to the greater geometrical irregularity which results in an increase in concentration polarization. In addition, intensive studies of the porous electrode have revealed additional experimental characteristics that are controversial. For example, Yeager and co-workers (3), using the interrupter technique, have observed polarization vs. current relationships during experiments on the oxygen-fed porous carbon electrode which show that the polarization depends on the resistance of the electrolyte. However, the accepted theory for the interrupter technique indicates that the resistive component of polarization should not be observable with this technique. This paper presents a theory for the porous electrode which includes the resistance of the electrolyte within the pores as well as concentration and activation polarization. The numerical results obtained with this theory are compared with experimental results.

THEORETICAL MODEL

The porous gaseous-diffusion electrode is analogous to a bundle of tubes of uniform radius and length. (4) In the actual porous electrode the tubes or pores are quite tortuous and nonuniform in structure and diameter. In addition they are interconnected. The small pores are flooded and only regions of large diameter have a sufficiently low capillary pressure to be maintained free of electrolyte at the prevailing differential pressure. It is proposed that the pore may be visualized in terms of a constricted tube as depicted in Figure 1. The reaction of the active gas occurs on the wall of the tube in the region of the thin meniscus where the electrolyte and gas are in contact. This active electrochemical area, called the diffuse three-phase zone, is small relative to the total surface of the pore. Electrolytic conduction exists through the length of the pore. In regions where the pore is constricted, there will be considerable current density and, consequently, an appreciable ohmic potential loss may occur. In this model, the pore region in the pore region in the part of the flooded porous structure adjacent to the main body of the electrolyte will be referred to as the mouth. The pore region in the part of the flooded porous structure adjacent to the gas phase will be referred to as the interior region. The constriction in the pore is assumed to separate the interior region and the mouth of the pore. All the resistance of all constrictions which become flooded when the differential gas pressure decreases is lumped into a single resistance,  $\rho$ , per unit area of electrode.

Fig. 1

# IDEALIZED MODEL OF ELECTRODE PORE

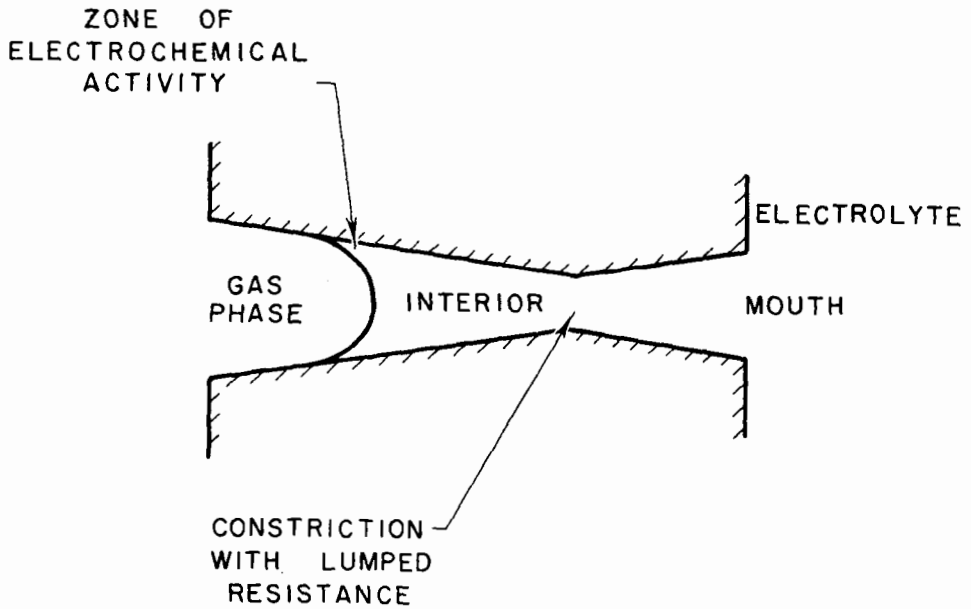
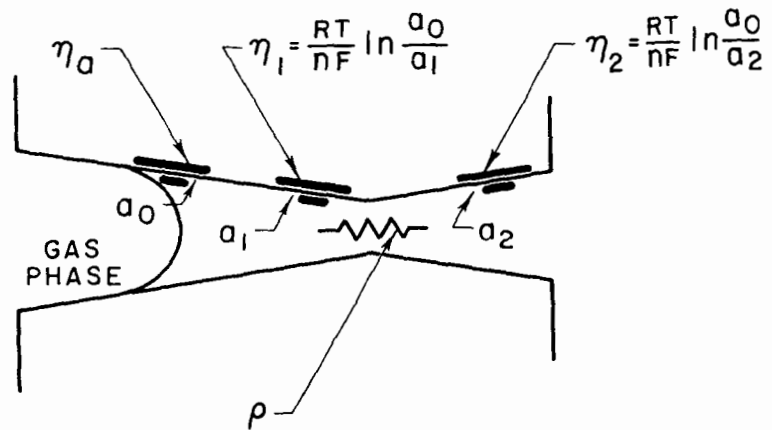


Fig. 2

## LOCATION OF ELECTRICAL ANALOGUES IN PORE



Normally, under open-circuit conditions, the area of the electrode wetted with electrolyte is uniformly covered with a layer of active gas. When a current is drawn which exceeds the flow rate of gas to the mouth, the active electrochemical area degenerates to the diffuse three-phase zone. Where loads are so small that diffusion and convection mechanisms are sufficiently rapid to replace the adsorbed gas which is discharged, the flat-plate model of the electrode becomes adequate. We are concerned here only with loads which result in an active electrochemical area restricted to the diffuse three-phase zone. Under such conditions, there will be a high concentration of active gas in this zone. It is assumed that the electrode is operated in a current range where the gas adsorbed on the surface in the diffuse three-phase zone is approximately in equilibrium with the gas phase. In this area a fixed activity,  $a_0$ , of gas is assumed. In the flooded interior of the pore, the equivalent gas-phase activity of the gas at the surface is  $a_1$ , while in the mouth of the pore the gas activity is  $a_2$ . With these activities, the following concentration potentials exist:

$$\eta_1 = \frac{RT}{nF} \ln \frac{a_0}{a_1} \quad (1a)$$

$$\eta_2 = \frac{RT}{nF} \ln \frac{a_0}{a_2} \quad (1b)$$

where  $\eta_1$  is the concentration polarization existing in the interior of the pore,  
 $\eta_2$  is the concentration polarization in the mouth of the pore,  
 $R$  is the gas constant,  
 $T$  is the absolute temperature,  
 $n$  is the number of electrons involved in the electrochemical process and  
 $F$  is the charge equivalent of a gram-mole of electrons.

The discussion below may be generally applied to any gaseous electrode but let us consider, in particular, the hydrogen electrode in concentrated caustic. The value of the ratios of hydrogen activity may be as high as  $10^6$  for observed polarization values of 200 mv. Long periods of anodic operation of the hydrogen electrode result in the formation of an activity gradient due to the water formed. Because of the greater volume of space accessible to the water, the water activity ratio never becomes as significant as that of the hydrogen. For a 100% increase in water activity, a 10 mv change can be expected at 90°C. Since water is present in macroscopic quantities compared to surface concentrations of the gas, the decay of water concentration polarization would require much more time (other parameters being equal). For the following discussion we will assume that water concentration polarization is negligible.

When an external load is suddenly removed, the concentration potentials begin to discharge through the long pore. The concentration gradients may relax through normal diffusion of matter, but in fine capillary pores this process is extremely slow compared with electrochemical transport. For this discussion, relaxation of concentration gradients by diffusion is assumed to be insignificant. The discharge of the concentration gradients in the mouth of the pore is limited by resistance and activation polarization, whereas discharge in the interior of the pore is limited only by the activation polarization. The activation polarization is considered negligible in regions remote from the diffuse three-phase zone because the area is relatively large and the current density is extremely low. The equivalent electrical analog of the discharging process in the pore is shown in Figures 2 and 3. Although potential sources exist everywhere along the interface, for this discussion it is assumed that the potential sources are localized as in Figure 2. The activation polarization is represented by  $\eta_a$  and the capacitances of the double layer (assumed constant) are  $C_1$  and  $C_2$  associated with the interior and mouth portions of the pore, respectively. The equations of potential balance are

$$\eta_a = \eta_1 \quad (2)$$

$$\eta_a = \eta_2 - i_2 \rho \quad (3)$$

where  $i_2$ , the current in the resistive leg, is defined as the sum of the faradaic current through the potential source  $\eta_2$  and the capacitive current discharging from  $C_2$ .

Fig. 3

# SCHEMATIC DIAGRAM OF ELECTRICAL ANALOGUE OF PORE

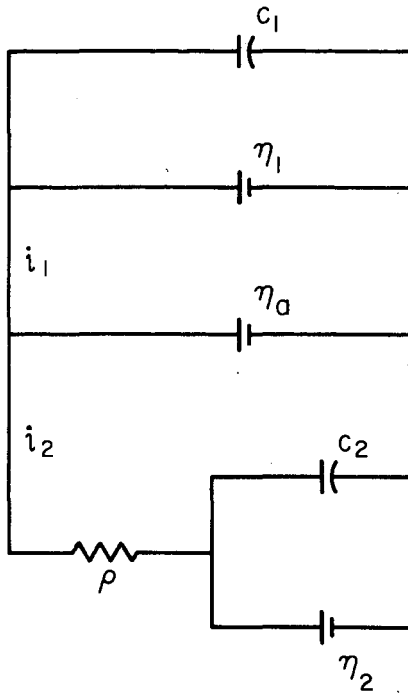
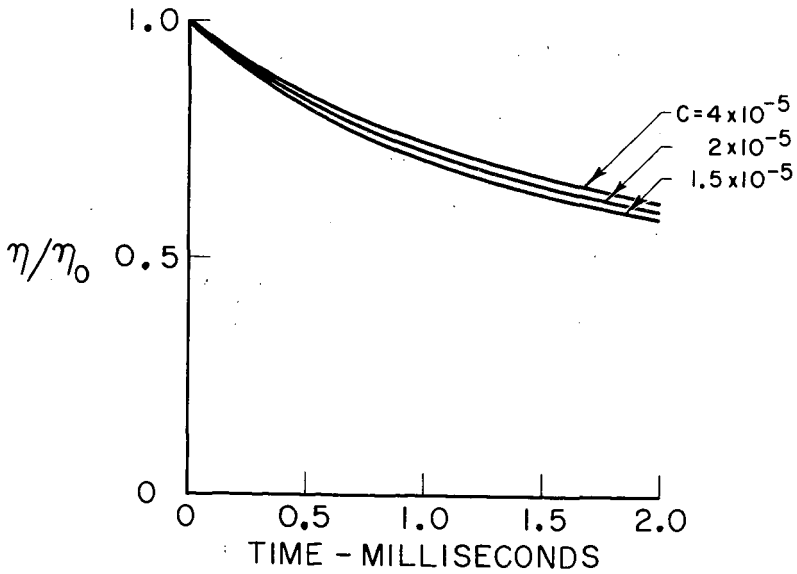


Fig. 4

## EFFECT OF C ON POLARIZATION



The current  $i_1$  is similarly defined, as the sum of the faradaic current through  $\eta_1$  and the current discharging from  $C_1$ .

$$i_1 = nF \frac{d(V_1 a_1)}{dt} - C_1 \frac{d\eta_1}{dt} \quad (4a)$$

$$i_2 = nF \frac{d(V_2 a_2)}{dt} - C_2 \frac{d\eta_2}{dt} \quad (4b)$$

where  $V_1$  and  $V_2$ , the equivalent volumes of gas per  $\text{cm}^2$  of surface area, represent the capacity of the surfaces in the interior and mouth of the pore for adsorption of the gas. In the case of discharge of hydrogen ions on a severely oxidized metal lattice, the equivalent volume may be very large. It is assumed that the activity of hydrogen in the mass of the solid heterogeneous oxide changes homogeneously and continuously. In numerical calculation, these volumes can be assumed to include both the equivalent volume of adsorbed gas and the volume of dissolved gas in the electrolyte contained in the appropriate region of the pore.

If the transmission coefficient is  $1/2$ , the equation relating activation polarization and current may be written

$$i_1 + i_2 = 2 i_0 \sinh \frac{nF\eta_0}{2RT} \quad (5)$$

where  $i_0$  is the exchange current. Equations (1) through (5) can be combined (see Appendix) to yield the following simultaneous, first-order, nonlinear, differential equations.

$$\frac{d\eta_2}{dt} = - \frac{\left( \frac{\eta_2 - \eta_1}{\rho} \right)}{C_2 + \frac{V_{a0} n^2 F^2}{RT} e^{-\frac{nF\eta_2}{RT}}} \quad (6)$$

$$\frac{d\eta_1}{dt} = - \frac{2 i_0 \sinh \frac{nF\eta_1}{2RT} + \frac{\eta_1 - \eta_2}{\rho}}{C_1 + \frac{V_{a0} n^2 F^2}{RT} e^{-\frac{nF\eta_1}{RT}}} \quad (7)$$

These equations are in a form suitable for solution on an analogue computer.

## RESULTS OF ANALOGUE COMPUTER CALCULATIONS

Equations (6) and (7) from the preceding section were used to determine the variation of polarization with time for various values of the parameters  $C$ ,  $V_{a0}$ ,  $i_0$ , and  $\rho$  occurring in these equations. The equations were solved using a Berkeley EASE Model 1032 analogue computer at the UAC Research Laboratories.

The values of parameters incorporated into the analogue computer program are listed below.

$n$  = 2 electrons/mole for the case of hydrogen

$F$  = 96,500 coulombs/gram-equivalent of electrons

$R$  = 8.314 joules/degree mole

$T$  = 460 deg K

$C_1 = C_2 = 1.5 \times 10^{-5}$  to  $4 \times 10^{-5}$  farad/ $\text{cm}^2$

$a_0 = 4.46 \times 10^{-5}$  moles/ $\text{cm}^3$  at STP conditions

Fig. 5

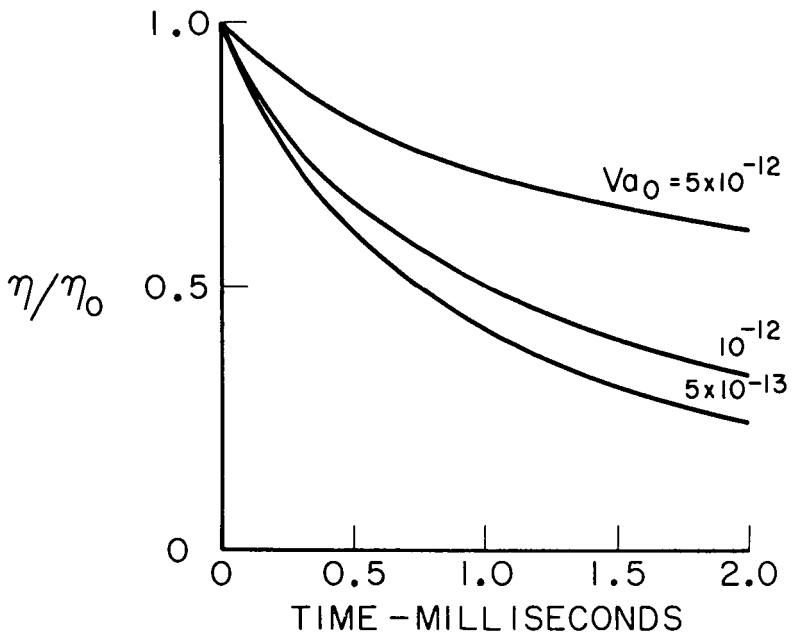
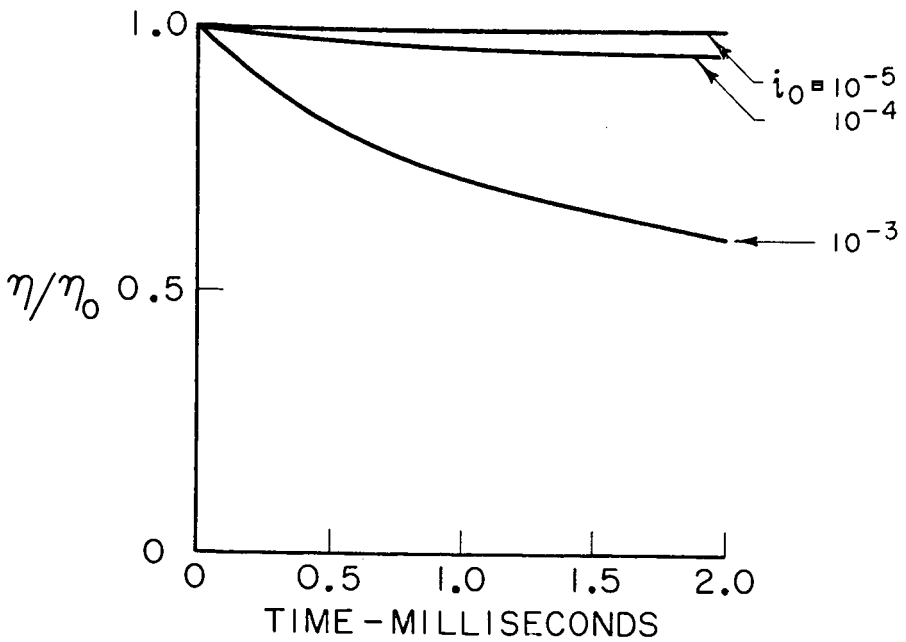
EFFECT OF  $Va_0$  ON POLARIZATION

Fig. 6

EFFECT OF  $i_0$  ON POLARIZATION

$$\rho = 5 \text{ to } 20 \text{ ohms}$$

$$i_0 = 10^{-3} \text{ to } 10^{-5} \text{ amp/cm}^2$$

$$V_1 = V_2 = 10^{-8} \text{ to } 10^{-7} \text{ cm}^3/\text{cm}^2 \text{ at STP conditions}$$

$$V_{O_0} = 5 \times 10^{-13} \text{ to } 5 \times 10^{-12} \text{ moles/cm}^2$$

The quantity,  $V$ , has units of length since it is volume per unit of area. It represents the effective thickness of the hydrogen-depleted zone to which hydrogen activity is being returned. If the zone is a bare metallic unoxidized surface, the length in question has dimensions of the hydrogen atom, namely  $10^{-8}$  cm. However, this length must be corrected by the molar volume ratio appropriate to the gaseous state which at atmospheric pressure is  $10^{-3}$  to  $10^{-2}$  times as dense as the adsorbed state. In addition, the surface coverage (5) by hydrogen in competition with an electrolyte such as KOH is only about 1% or less so that an additional factor of  $10^{-2}$  or less may be required. The resultant over-all  $V_{O_0}$  factor is  $4.46 \times 10^{-13}$  or less for the case of pure hydrogen adsorbed on an oxide-free surface. If, however, the surface is in a state of oxidation involving one to  $10^4$  oxide layers, then the oxide layer may be up to  $10^{-4}$  cm in thickness and the resultant over-all  $V_{O_0}$  factor may range from  $4.46 \times 10^{-6}$  to  $4.46 \times 10^{-12}$  moles/cm<sup>2</sup> or less. The values used in the computer program are representative of the moderately low range, namely  $5 \times 10^{-13}$  to  $5 \times 10^{-12}$ .

The variation of polarization for various values of the parameters  $C$ ,  $V_{O_0}$ ,  $i_0$ , and  $\rho$  is shown in Figures 4 through 7. The effects of  $C$  and  $V_{O_0}$  are closely inter-related because of their simultaneous occurrence in the denominators of Equations (6) and (7). If the exponential term is large relative to the initial value of  $C$  there is negligible effect until  $C$  approaches the magnitude of the exponential. For the value of the variables used in these calculations, the effect of increasing  $C$  is to decrease the initial slope and reduce the curvature as shown in Figure 4.

The effect of the magnitude of  $V_{O_0}$  is influenced by the rapidly changing exponential factor. At low polarization values and high values of  $V_{O_0}$  the capacitance term becomes negligible and the exponential term decreases the slope and increases the flatness of the long time decay portion of the curve as shown in Figure 5.

For a given polarization, increasing  $i_0$  causes the slope of the initial portion of the polarization decay curve to increase. This variation is shown in Figure 6. This may also be seen analytically: when  $C$  is large compared to the exponential term, Equations (6) and (7) can be combined to give

$$\frac{d\eta_2}{dt} + \frac{d\eta_1}{dt} \cong - \frac{2 i_0 \sinh \frac{nF\eta_1}{2RT}}{C + \frac{V_{O_0} n^2 F^2}{RT} e^{-\frac{nF\eta_1}{2RT}}} \quad (8)$$

The effect of increasing  $\rho$  is similar to the effect of increasing  $C$  and  $V_{O_0}$  simultaneously. Figure 7 shows the calculated family of curves obtained by varying  $\rho$ .

In general, the calculated decay curves shown in Figures 4 through 7 fall off slowly and at a given time the values of polarization are substantially above the values predicted by Grahame (1) for his highly simplified model (see Figure 8). For the case where  $i_0$  is  $10^{-3}$  amp/cm<sup>2</sup>,  $C$  is  $2 \times 10^{-5}$  farad/cm<sup>2</sup>,  $V_{O_0}$  is  $10^{-12}$  moles/cm<sup>2</sup> and  $\rho$  is 10 ohms, the theory presented herein predicts a 50% decay in polarization during the first millisecond. For the same  $i_0$ , and  $C$ , Grahame's results which neglect concentration changes predicts a 90% decay in polarization after one millisecond.

## DISCUSSION

A quantitative comparison of the theory developed in this paper with results obtained experimentally is extremely difficult because of the problems that arise in precise evaluation of such parameters as  $C$  and  $V_{O_0}$  in an experimental electrode. However, the qualitative comparison of theoretical and experimental results is not difficult. Experimental data for a hydrogen electrode in a KOH cell operating at temperatures of approximately 190°C. were obtained at the UAC Research Laboratories.

Fig. 7  
EFFECT OF  $\rho$  ON POLARIZATION

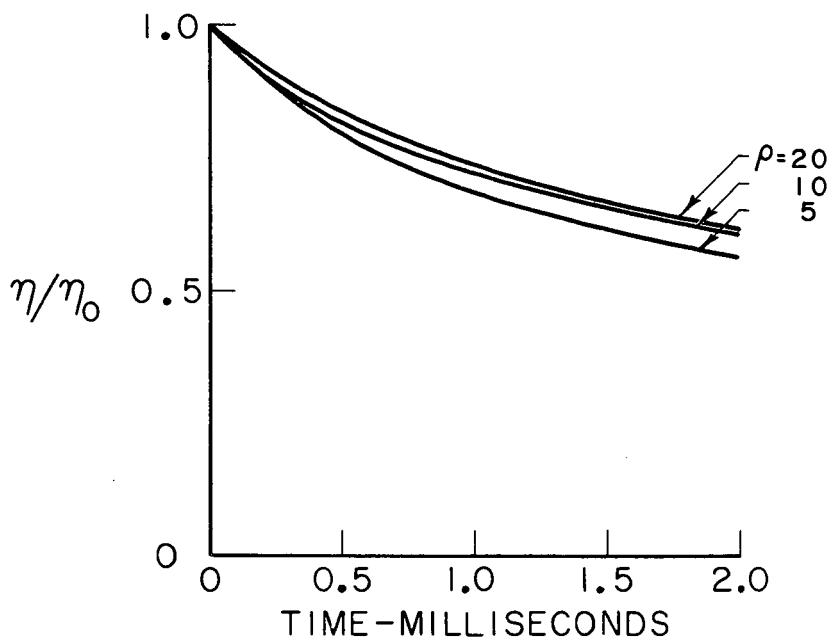
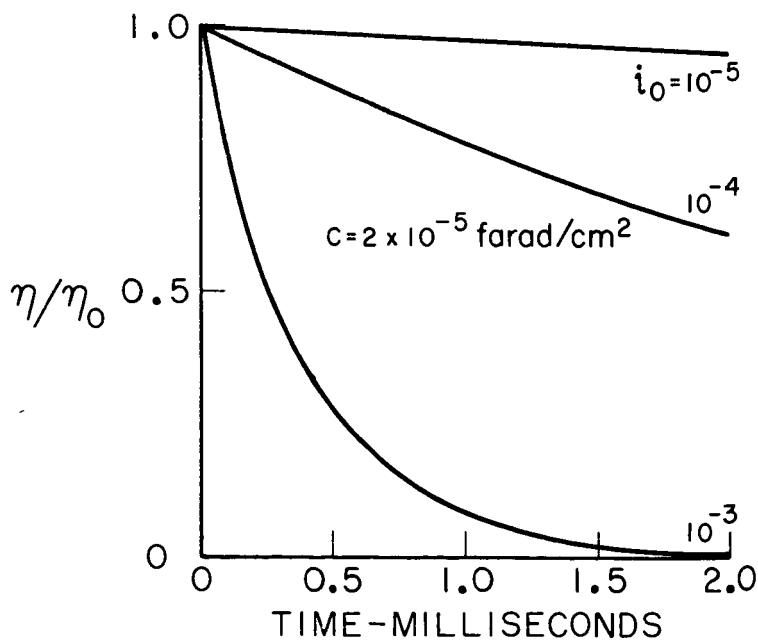


Fig. 8  
THEORETICAL DECAY OF POLARIZATION FOR  
FLAT PLATE WITH NO CONCENTRATION CHANGE





Representative decay curves from these experiments are shown in Figure 9. The shape of these curves is similar to that of the experimental results reported in Reference 6. The most significant feature of these curves is their relatively slow decay (less than 25% for times less than 1 millisecond). This feature is reproduced qualitatively by the theory presented herein as indicated by the theoretical curve shown in Figure 9 which is plotted for a value of  $i_0$  equal to  $10^{-3}$  amps/cm<sup>2</sup>. The values of  $i_0$  for the experimental data were estimated by combining the values of  $i_2$  and  $\eta_2$  observed experimentally with an experimental value of  $\rho$  (of the order of 5 ohms) in Equations (3) and (5). The value of  $i_0$  for the limiting case of zero resistance (corresponding to  $\eta_2 = \eta_1$ ) was also calculated. In all cases the estimated values of  $i_0$  were found to be between  $10^{-2}$  and  $10^{-3}$  amps/cm<sup>2</sup>. The values calculated using the theory proposed in this paper are obviously in better agreement with the experimental data than are those of Grahame. (If the theoretical curve for  $i_0 = 10^{-2}$  amps/cm<sup>2</sup> had been plotted instead, the agreement with the present theory would not have been as good but the agreement with results calculated from Grahame's theory would have been much worse). Although the theory presented herein is in reasonable agreement with the experimental results, it is obvious that the shape of the experimental curve is not satisfactorily reproduced. The major point of difference between the theoretical and experimental curves is in the relatively fast initial decay coupled with an abrupt change in slope during the first 0.1 millisecond for the experimental case. This abrupt change indicates that two decay processes are operative initially and that one relaxation process is relieved in a short time. It is believed that this process can be accounted for in the theory by removing the assumption that  $q_0$  is constant. By considering the relaxation time for  $q_0$  to recover to its equilibrium value, closer agreement between theory and experiment should result.

The Resistivity Effect - The shift of the polarization decay curve with change in resistivity of the electrolyte, as indicated in Figure 7, shows that the proposed theoretical model is able to predict a resistivity effect of the type suggested in Reference 3. Further insight into the implication of Equation (3), which is derived from the model, may be obtained if this equation is rearranged in the form

$$\eta_2 = \eta_0 + i_2 \rho \quad (3a)$$

In this form, Equation (3a) can be interpreted as indicating that the observed polarization is a simple addition of a pure activation polarization and a pure ohmic potential loss in the manner of Figure 10. The possibility that such a relation might exist was originally suggested by Yeager. (3) The experimental data of Urbach and Witherspoon (7) lend support to this hypothesis. Figure 11 taken from Reference 7 shows that the cathodic polarization curves of oxygen on carbon electrodes in solutions of potassium hydroxide of varying concentration go through a minimum at 5M KOH at which concentration the conductivity is a maximum. Figure 12 from the same reference shows the different cathodic polarizations for oxygen on carbon electrodes in equal concentrations of sodium and potassium hydroxide. In the potassium hydroxide solution, which is the better conductor, the polarization is lower.

In view of the theory presented here, it is seen that the interrupter technique can reveal an ohmic component of the polarization drop when the external current path is broken because an internal current through the pore continues to flow until the polarization has completely decayed and the ohmic loss must therefore become a component of the observed polarization as shown by Equation (3a). A rough quantitative check on the validity of Equation (3a) can be obtained by examining the polarization vs current curves of Figure 12 for large values of the cell current. The ratio of slopes under these conditions should approximate the resistivities of the electrolytes since, for large values of current

$$\frac{\eta_2}{i_2} = \frac{\eta_0}{i_2} + \rho \cong \rho \quad (9)$$

In the experimental data of Figure 12, the ratio of slopes for high current densities is 1.3 whereas the ratio of resistivities of sodium and potassium hydroxide is 1.55. The relationship between the ratio of slopes and the ratio of resistivities is good since the ratio of the slopes should be on the low side except in the limit, as indicated by the expression

Fig.9

## EXPERIMENTAL POLARIZATION DECAY VS TIME

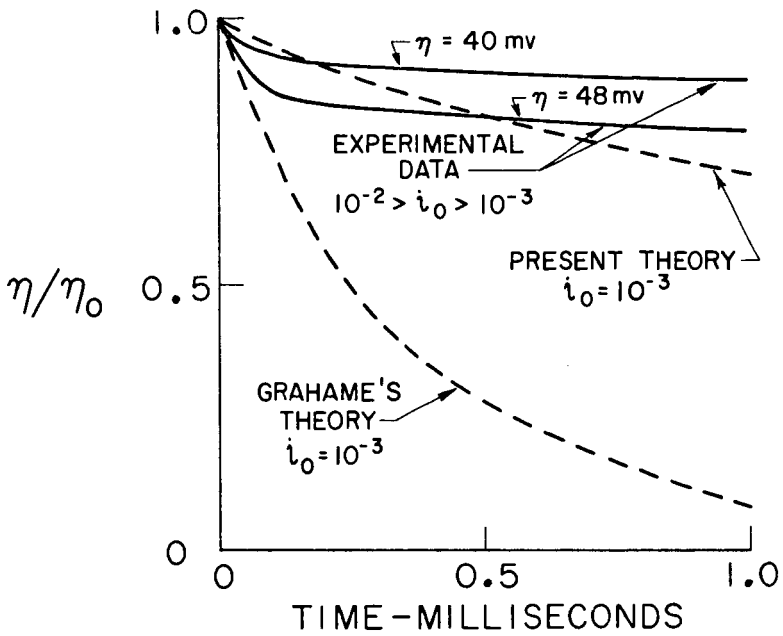
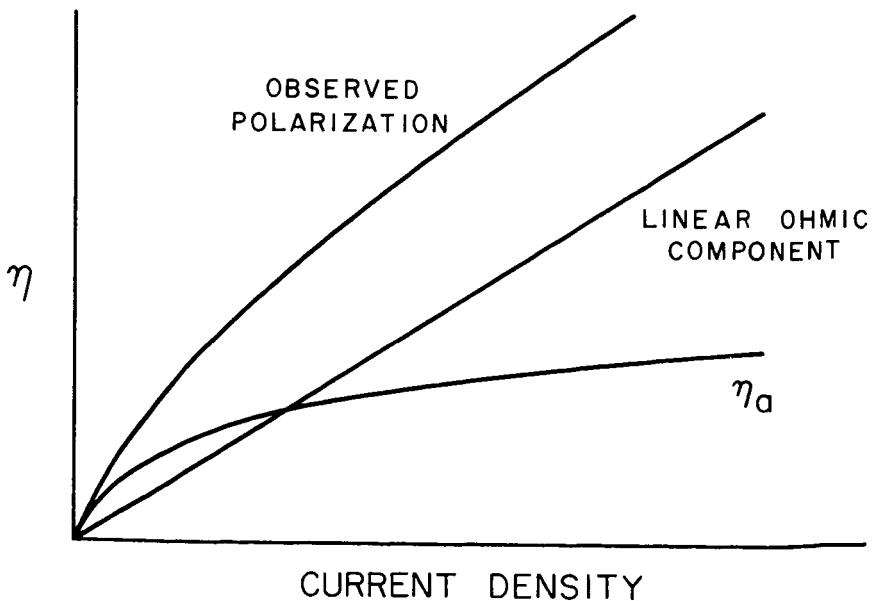


Fig. 10

COMPONENTS OF OBSERVED POLARIZATION  
IN POROUS ELECTRODE

$$\frac{\frac{\eta_0}{i} + \rho_{\text{NaOH}}}{\frac{\eta_0}{i} + \rho_{\text{KOH}}} < \frac{\rho_{\text{NaOH}}}{\rho_{\text{KOH}}} \quad (10)$$

The resistivity effect permits one to write the concentration polarization as the sum of a pure activation polarization and a pure ohmic potential loss factor. This relation is possible only for a concentration polarization within the pore. Concentration polarization outside the pore must be regarded in the classical manner.

Flat Plate as a Special Case of the Porous Electrode - The equations derived from the model postulated herein can be reduced to those of Grahame (1) in the special case where the resistivity,  $\rho$ , of the electrolyte approaches zero. In this case Equation (3) can be written

$$\eta_0 = \eta_2 \quad (11)$$

From Equations (2), (3), (6), and (7), we can therefore deduce (see Appendix)

$$\frac{d\eta}{dt} = - \frac{2 i_0 \sinh \frac{nF\eta}{2RT}}{C + \frac{V_{a0} n^2 F^2}{RT} e^{-\frac{nF\eta}{RT}}} \quad (12)$$

If, in Equation 12,  $V_{a0}$  is representative of a clean unoxidized surface, then the coefficient of the exponential term is negligibly small and we obtain an equation identical in form with Grahame's (1) expression for the flat plate electrode.

The integration of Equation (12) yields

$$2 V_{a0} nF \left( e^{-\frac{nF\eta}{2RT}} - e^{-\frac{nF\eta_0}{2RT}} \right) + \left( V_{a0} nF + \frac{RTC}{nF} \right) \ln \frac{\tanh \frac{nF\eta}{4RT}}{\tanh \frac{nF\eta_0}{4RT}} = -i_0 t \quad (13)$$

The constant  $\eta_0$  is the initial polarization. If the concentration polarization has been negligible  $V_{a0}$  becomes extremely small. Therefore, the exponential term in the denominator of Equation (12) may be neglected and Grahame's integrated form can be obtained (Equation 14).

$$\frac{RTC}{nF} \ln \frac{\tanh \frac{nF\eta}{4RT}}{\tanh \frac{nF\eta_0}{4RT}} = -i_0 t \quad (14)$$

Equation (14) was based on the assumption of unchanging concentrations in Grahame's (1) paper. Equation (13) can be extended to the flat plate case if it is assumed that some areas of the flat plate are more anodic than others so that they suffer a slight drift away from the equilibrium concentration of adsorbed hydrogen when under heavy external loads. The more sluggish areas of the electrode may be presumed to possess the equilibrium concentration of matter. If concentrations change, then the integrated form, Equation (13), may represent the polarization decay where the exponential factor is appreciable.

Effect of Change in the Differential Pressure Across an Electrode - One of the practical problems associated with the development of porous electrodes is the determination of the optimum operating pressure drop across an electrode. Experimentally it has been noted that the polarization increases as the differential pressure across an electrode decreases. This effect is qualitatively explained by the present theory on the grounds that the decrease in pressure increases the flooding of the pores and thereby increases the lumped resistance of the electrolyte. Hunger's (4) theory of electrode current limited by the viscous flow of gas through the pore predicts that the current density should be related to the square of the differential pressure. It would seem that a resistive term might be included in Hunger's (4) theory to account for additional current limitation by the ohmic factor.

Fig. 11

## EFFECT OF CONDUCTIVITY ON POLARIZATION

REFERENCE 7

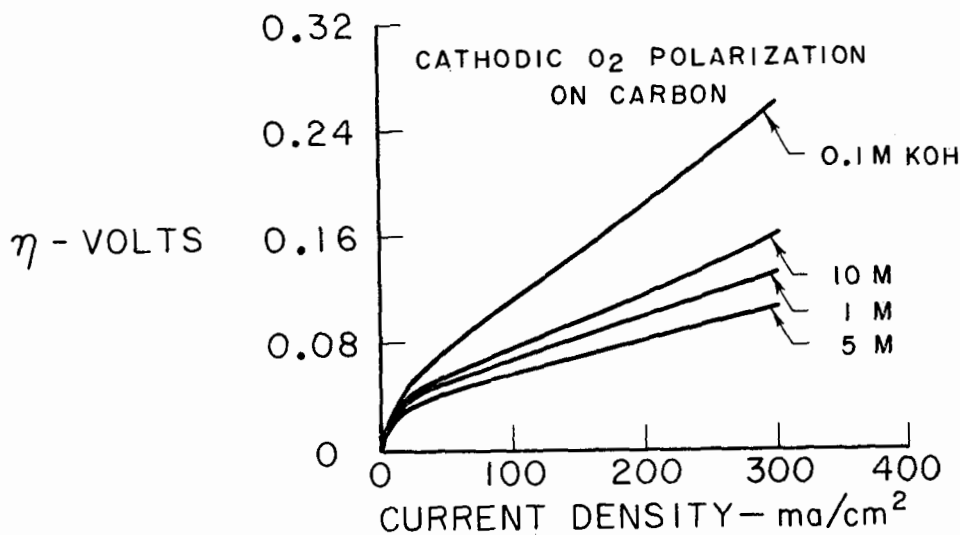
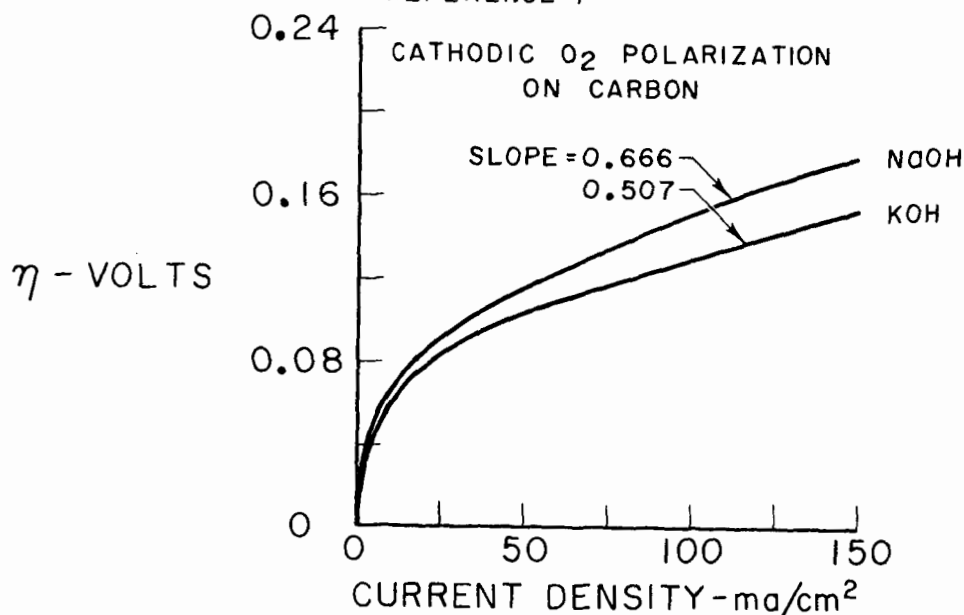


Fig. 12

EFFECT OF CONDUCTIVITY ON POLARIZATION  
EQUAL IONIC STRENGTH

REFERENCE 7



Effect of Increasing the Number of Pores - The present state of porous sintered electrode technology does not permit an unlimited increase of the number of pores within an electrode without concomitant reduction in the diameter of the pores. While the active area may increase with increased numbers of pores, the ohmic-loss factor must also simultaneously increase so that a minimum may be expected in the function relating electrode polarization and pore size.

## CONCLUSIONS

A model of the porous electrode has been presented which provides a basis for calculating polarization decay curves for electrodes which have significant amounts of concentration polarization in the pore. Comparison of theoretical and experimental curves shows qualitative agreement between the long-time values of polarization. In particular, the inclusion of concentration polarization eliminates the extremely rapid decay of polarization which was obtained in earlier theoretical studies. (1) The model gives rise to a quantitative relation between the observed polarization and the ohmic potential loss which is in agreement with some experimental data and concepts suggested by Yeager. (3) Finally, the treatment indicates that concentration polarization inside a pore behaves as the sum of a pure ohmic potential loss and a pure activation polarization.

## APPENDIX

The basic Equations (1) through (5) lead to the results of Equations (6) and (7) as shown below.

Eliminating  $\eta_d$  from Equations (2) and (3) it follows that

$$i_2 = \frac{\eta_2 - \eta_1}{\rho} \quad (15)$$

Eliminating  $i_2$  from Equations (4b) and (15) it follows that

$$nF \frac{d(V_2 a_2)}{dt} - C_2 \frac{d\eta_2}{dt} = \frac{\eta_2 - \eta_1}{\rho} \quad (16)$$

Equation (1b) can be rearranged and differentiated.

$$\frac{da_2}{dt} = -\frac{a_0 nF}{RT} e^{-\frac{nF\eta_2}{RT}} \frac{d\eta_2}{dt} \quad (17)$$

The volume,  $V_2$ , is constant and  $\frac{da_2}{dt}$  can be eliminated from Equation (16) with the expression (17).

$$-\left( \frac{V_2 a_0 n^2 F^2}{RT} e^{-\frac{nF\eta_2}{RT}} + C_2 \right) \frac{d\eta_2}{dt} = \frac{\eta_2 - \eta_1}{\rho} \quad (18)$$

Equation (6) is a rearrangement of Equation (18).

Equations (4a) and (4b) may be added to yield that the total current.

$$i_1 + i_2 = nF \frac{d(V_1 a_1)}{dt} + \frac{nF d(V_2 a_2)}{dt} - C_1 \frac{d\eta_1}{dt} - C_2 \frac{d\eta_2}{dt} \quad (19)$$

If Equation (2) is multiplied by  $\frac{nF}{2RT}$ , and the hyperbolic sine of each member is taken, then using Equation (5) one obtains

$$\frac{i_1 + i_2}{2 i_c} = \sinh \frac{nF \eta_1}{2RT} \quad (20)$$

Using (17) and the analogous equation for  $\eta_1$  Equation (19) can be written

$$i_1 + i_2 = -\frac{V_1 a_0 n^2 F^2}{RT} e^{-\frac{nF\eta_1}{RT}} \frac{d\eta_1}{dt} - \frac{V_2 a_0 n^2 F^2}{RT} e^{-\frac{nF\eta_2}{RT}} \frac{d\eta_2}{dt} - C_1 \frac{d\eta_1}{dt} - C_2 \frac{d\eta_2}{dt} \quad (21)$$

Using (21) to eliminate  $i_1 - i_2$  Equation (20) can be written

$$-\left(\frac{V_1 a_0 n^2 F^2}{RT} e^{-\frac{nF\eta_1}{RT}} + C_1\right) \frac{d\eta_1}{dt} - \left(\frac{V_2 a_0 n^2 F^2}{RT} e^{-\frac{nF\eta_2}{RT}} + C_2\right) \frac{d\eta_2}{dt} = 2 i_0 \sinh \frac{nF\eta_1}{2RT} \quad (22)$$

The derivative of  $\eta_2$  with its coefficient can be eliminated through (18) so that

$$-\left(\frac{V_1 a_0 n^2 F^2}{RT} e^{-\frac{nF\eta_1}{RT}} + C_1\right) \frac{d\eta_1}{dt} + \frac{\eta_2 - \eta_1}{\rho} = 2 i_0 \sinh \frac{nF\eta_1}{2RT} \quad (23)$$

Equation (23) is a rearrangement of Equation (7).

Equation (11) leads to Equation (12) in the following manner. In Equation (5) we write  $i$  for  $(i_1 - i_2)$  and using Equation (4a) without subscripts we eliminate the current.

$$nFV \frac{da}{dt} - \frac{C d\eta}{dt} = 2 i_0 \sinh \frac{nF\eta}{2RT} \quad (24)$$

Using Equation (17)  $\frac{da}{dt}$  can be eliminated to yield (25) which is a form of (12).

$$-\left(\frac{V a_0 n^2 F^2}{RT} e^{-\frac{nF\eta}{RT}} + C\right) \frac{d\eta}{dt} = 2 i_0 \sinh \frac{nF\eta}{2RT} \quad (25)$$

Equation (12) can be rearranged and integrated to give

$$\int_{\eta_0}^{\eta} \frac{\left(\frac{V a_0 n^2 F^2}{RT} e^{-\frac{nF\eta}{RT}} + C\right)}{\sinh \frac{nF\eta}{2RT}} d\eta = -2 i_0 \int_0^t dt \quad (26)$$

The exchange current is relatively unaffected by changes in concentration since  $a_0$  was assumed constant. The left member of (26) can be broken into a sum of integrals.

$$C \int \operatorname{csch} \frac{nF\eta}{2RT} d\eta + \frac{V a_0 n^2 F^2}{RT} \left[ - \int e^{-\frac{nF\eta}{2RT}} d\eta + \frac{1}{2} \int \frac{e^{-\frac{nF\eta}{2RT}}}{1 + e^{-\frac{nF\eta}{2RT}}} d\eta + \frac{1}{2} \int \frac{e^{-\frac{nF\eta}{2RT}}}{1 - e^{-\frac{nF\eta}{2RT}}} d\eta \right] = -2 i_0 t \quad (27)$$

When the integration is performed the result is Equation (13).

$$2V_0 nF \left( e^{-\frac{nF\eta}{2RT}} - e^{-\frac{nF\eta_0}{2RT}} \right) + \left( V_0 nF + \frac{RTC}{nF} \right) \ln \frac{\tanh \frac{nF\eta}{4RT}}{\tanh \frac{nF\eta_0}{4RT}} = -i_0 t \quad (13)$$

#### ACKNOWLEDGMENT

The author wishes to express his appreciation to Mr. D. G. McMahon for his helpful criticism and discussion. In addition, he extends his thanks to Mr. Frank Scanlon for his assistance in the analogue computation.

#### LITERATURE CITED

- (1) Grahame, D. G., *J. Phys. Chem.*, **57**, 757 (1953).
- (2) Scott, T., *J. Chem. Phys.*, **23**, 1936 (1955).
- (3) Urbach, H. B., Witherspoon, R. R., and Yeager, E., Abstracts of the Spring Meeting of the American Chemical Society, New York, N. Y., April, 1953.
- (4) Hunger, H., USASRD Technical Report 2001, AD-219732, December 15, 1958.
- (5) Schuldiner, S., *J. Electrochem. Soc.*, **106**, 891 (1959).
- (6) Armstrong, G., and Butler, J. A. V., *Trans Faraday Soc.*, **29**, 1261 (1933).
- (7) Urbach, H., and Witherspoon, R. R., Thesis, "Kinetics of the Oxygen Electrode". Western Reserve University, Cleveland, Ohio, October 1953.